JOURNAL OF CATALYSIS **142**, 312–324 (1993)

The Use of DRIFTS-MS and Kinetic Studies to Determine the Role of Acetic Acid in the Palladium-Catalyzed Vapor-Phase Synthesis of Vinyl Acetate

STEVE M. AUGUSTINE[1] AND JONATHAN P. BLITZ

Allen Research Center, Quantum Chemical Corporation, Cincinnati, Ohio 45249

Received December 11, 1992; revised February 16, 1993

Supported palladium catalyzes the synthesis of vinyl acetate (VA) by oxyacetylation of ethylene. Alkali promoters increase activity and selectivity. The role of acetic acid (HOAc) in these processes is not well understood. Activation energy studies show that HOAc alters the catalyst site and lowers the reaction barrier to VA formation. After correction for this effect, the kinetics reveal that as a reagent HOAc is zero order. This is probably due to a strong adsorption of HOAc on Pd which forms the catalyst active phase. Detailed spectroscopic studies support this conclusion. The surface processes on a supported vinyl acetate catalyst were studied using a method which couples diffuse reflectance infrared Fourier transform spectroscopy (DRIFTS) with mass spectrometry (MS). The DRIFTS–MS technique combines the capability of selectively analyzing IR-active surface species with sensitive detection of transient reaction products. By comparing the catalyst with mixtures of palladium acetate powder physically dispersed in potassium chloride, it is determined that the active phase on the catalyst is a form of palladium acetate. Compound formation is consistent with the strong chemisorption of HOAc on Pd. Kinetic analysis of temperature-programmed reaction (TPRxn) data suggests that Pd metal or metal oxide adjacent to the active site is important in the reaction mechanism.

INTRODUCTION

It has been known for nearly 30 years that the oxyacetylation of ethylene to form vinyl acetate is catalyzed by supported Pd and Pd alloys (*3*). The reaction is written as

$$C_2H_4 + CH_3COOH + \tfrac{1}{2}O_2 \rightarrow C_2H_3OOCCH_3 + H_2O.$$

Despite the maturity of the process, disagreement still exists over the reaction kinetics and mechanism. Studies on this subject differ on the kinetic order of HOAc in the reaction with reported values varying from 0 (*4, 5*) to 0.5 (*6*) to 1 (*7*). Acetic acid's precise role in altering the catalyst surface is also disputed (*4, 8*).

The vinyl acetate catalyst system employs several IR-active chromophores. In addition to HOAc, ethylene, and VA, the catalysts are often promoted with alkali acetate salts. As such, the system lends itself well to analysis using a reactor system combining diffuse reflectance infrared with mass spectrometry. By its nature, DRIFTS is a reflectance technique, and thus preferred over transmission FTIR because of its greater surface selectivity (*9*). A controlled atmosphere, variable temperature DRIFTS cell serves as both an IR cell and a reactor. Coupling a mass spectrometer to the effluent aids in the assignment of bands to surface species directly associated with reaction products.

We have used the DRIFTS–MS technique to determine the role of acetic acid on the catalyst surface in this reaction. Data from activation energy, kinetic, and temperature-programmed reaction studies serve to support these findings.

---

[1] To whom correspondence should be addressed.

0021-9517/93 $5.00

METHODS

A. Catalyst and Reagents

The catalyst consists of Pd supported on α-alumina. It is prepared according to Ref. (*10*). It has a nominal Pd loading of 1.2 wt% and is promoted with a mixture of $KC_2H_3O_2$ (KOAc) and KOH.

Two model systems are also investigated. The first consists of a 5% $Pd(C_2H_3O_2)_2$ ($Pd(OAc)_2$; 98% purity) physically dispersed in KCl (<99.9%) or KOAc. The KCl is ground with a mortar and pestle and then in a Wig-L-Bug for 2 min. The sample is dried for 48 hr at 140°C prior to grinding with $Pd(OAc)_2$ in the Wig-L-Bug. The second model is prepared by first dissolving 0.2 g $Pd(OAc)_2$ in 15 ml methanol. The solution is added to 2 g of the Pd catalyst described above. The mixture is dried in a rotary evaporator under vacuum at room temperature.

Ethylene (>99.9%), oxygen (>99.98%), and helium (>99.99%) are all dried with 5A molecular sieve prior to use. Glacial acetic acid is used as received. It is placed in a variable temperature sparger through which the gas mixture is passed and saturated.

B. Procedures

B1. Temperature-programmed reactions. Temperature-programmed reaction studies are performed in both the DRIFTS–MS unit and a differential microreactor to obtain both qualitative and quantitative analyses, resp. Both systems are run at atmospheric pressure.

The DRIFTS–MS unit couples a Dycor quadrupole mass spectrometer to the vent line of a Harrick, controlled atmosphere, variable temperature diffuse reflectance cell. The spectra are taken with a Nicolet 60SX FT-IR spectrometer equipped with a narrow-band MCT detector. The details of the equipment setup and experimental methods are presented elsewhere (*2*); see also (*1*).

The microreactor is designed to combine C_2H_4, O_2, and He prior to saturating the gas stream with HOAc in a variable temperature sparger. The entire reactor is enclosed in an oven and operated at elevated temperatures to prevent condensation of HOAc and VA. A heated, 100-μm capillary taken from the vent of the reactor and run to a Dycor M200 mass spectrometer allows continuous effluent analysis. The mass spectrometer and an LFE temperature programmer are directly interfaced with a computer for data collection.

TPRxn results are obtained by first bringing the catalyst to steady state at 140°C with a reaction mixture of 88.6% C_2H_4, 9.8% O_2, and 1.6% HOAc. The total flow rate is 102 ml/min. At this point ethylene is replaced by a diluent gas (either N_2 or He), and the catalyst is kept under these temperature and flow conditions for 30 min. Both HOAc and O_2 are then replaced by diluent, and the pretreatment continues until the HOAc response in the mass spectrometer reaches background levels. The reactor is then cooled prior to the TPRxn.

The TPRxn's are run from 30°C with a temperature ramp of 10°C/min. The reaction gas mixture is 90% C_2H_4 and 10% O_2. The total flow rate is 100 ml/min. Mass spectra are collected every 6 sec. The mass spectrometer is calibrated after each run.

In the DRIFTS–MS studies the DRIFTS cell is filled with pure catalyst or a mixture of 5% $Pd(OAc)_2$ in KCl. The use of pure catalyst is necessary to ensure product formation above the sensitivity limits of the mass spectrometer. The use of pure catalyst eliminates the possibility of obtaining quantitative information with the DRIFTS technique. Therefore as a matter of uniformity, all spectral data are calculated using the Beer–Lambert law. Although not quantitatively accurate, qualitative trends can still be followed as "apparent absorbance" units (*11*). The sample height is optimized in all cases by maximizing the interferogram centerburst at 110°C to minimize the effects of a change in sample height with temperature (*12*). Either 16 or 32 scans are averaged at 4 cm^{-1} nominal resolution. Spectral acquisition is done every 10°C and requires 5–10

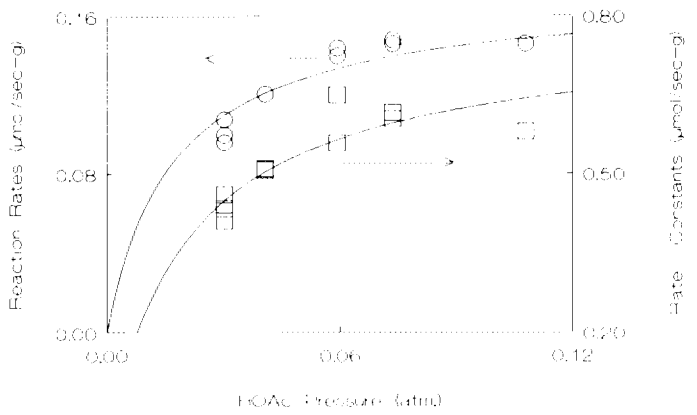

FIG. 1. Rate of vinyl acetate formation as a function of acetic acid partial pressure. Circles represent measured reaction rates and squares represent calculated rate constants.

sec. Single-beam spectra are ratioed to pure KCl.

B2. Kinetic studies. Reaction kinetics and activation energies are determined in the microreactor. In these reactions the HOAc composition of the reactant feed stream is varied from 3–11%. The total gas flow is ca. 105 ml/min with ethylene making up 80% and oxygen comprising 9%. Where necessary, He is used to make up the balance.

The activation energy studies are fully automated and begin by establishing steady state at 140°C. Data is then collected successively at 150, 130, 155, and 125°C. The reaction is returned to 140°C to ensure that catalyst performance is not significantly altered by the cycle. The mass spectrometer is calibrated at the end of each run. Baseline studies are done with finely ground samples and samples ground and mixed with blank Al_2O_3 to see if the reaction is either pore or film diffusion controlled, resp. (*13*). In both cases the results are within experimental error of the regularly treated sample. Therefore, diffusion is not a problem. The kinetic data reported in Fig. 1 are averages of the 140°C results.

RESULTS AND DISCUSSION

A. Kinetics

The rate of vinyl acetate formation over a Pd catalyst as a function of acetic acid partial pressure is presented in Fig. 1. These results agree with those reported previously (*4, 7*). At first glance, the reaction appears to be governed by saturation kinetics. These data can be described by a first-order Langmuir–Hinshelwood approximation (*14*). However, further analysis shows that this is not the true case (see below).

Arrhenius data show that increasing HOAc pressure will lower the apparent activation energy of the reaction (Fig. 2). Raising HOAc pressure from 0.03 atm to 0.11 atm causes the vinyl acetate activation energy to drop almost 5 kcal/mol (Table 1). The indication is that excess HOAc alters the catalyst active site causing a reduction in the reaction barrier.

Acetic acid seems to be playing two different roles which influence the rate of this reaction. The first is to alter the energetics of the active site and lower the activation barrier. HOAc is also a reagent, and as such it may also possess a nonzero order in the kinetic rate law. The former influences the exponent of the kinetic rate law, thus it should exert the largest influence and may overshadow the latter. For this reason the reaction order of HOAc was determined with a multivariable linear regression analysis of the available kinetic data. This model takes both factors of activation energy and reaction order into account, but one as-

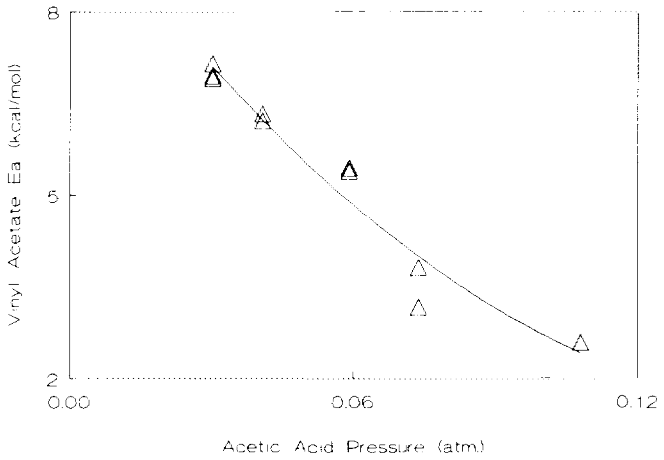

FIG. 2. Activation energy for the formation of vinyl acetate versus acetic acid partial pressure.

sumption needs to be made. If the reaction follows a typical kinetic rate law,

$$\frac{d[\mathrm{VA}]}{dt} = A\exp(-E_a/RT) \times \left(\prod_i [\mathrm{R_i}]^{x_i}\right)[\mathrm{HOAc}]^{y},$$

where

A = Kinetic preexponential factor.

E_a = Reaction apparent activation energy.

R = Ideal gas constant.

T = Reaction temperature.

$[\mathrm{R_i}]$ = Concentration of reagent i, either O_2 or C_2H_4.

x_i = Reaction order of reagent i.

y = Reaction order of HOAc.

Then we need to assume that some kind of compensation effect is occurring between the reaction activation energy and the preexponent (*15*),

$$\ln(A) = mE_a + \ln(k'),$$

where m is the degree of the compensation or the slope, and k' is the value of A when there is no barrier. A compensation effect

TABLE I

Reaction Rate Parameters as Functions of Acetic Acid Partial Pressure

Acetic partial pressure	Activation energy (kcal/mole)	Ln(A)	Observed rate (μmole/g-sec)	Rate constant (μmole/g-sec)
0.030	7.15	7.82	0.0966	0.410
	6.95	7.68	0.108	0.460
	6.91	7.57	0.100	0.433
0.041	6.33	6.89	0.121	0.508
	6.21	7.04	0.121	0.510
0.059	5.45	6.06	0.144	0.560
	5.39	6.14	0.144	0.652
0.074	3.80	4.15	0.148	0.618
	3.16	3.35	0.146	0.606
0.11	2.58	2.60	0.137	0.581

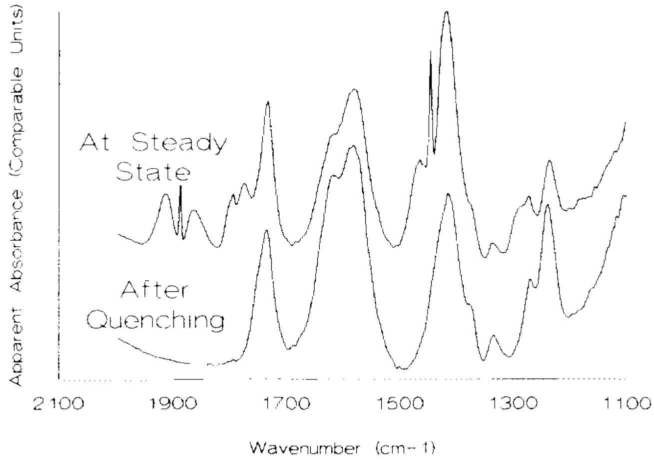

FIG. 3. Diffuse reflectance infrared spectra of an active catalyst surface. The upper spectrum is taken at steady state. The lower spectrum is taken after quenching the reaction by replacing the reagents with nitrogen as outlined in the Methods section.

must be occurring since the change observed in the activation barrier alone should alter the rate by a factor of 262 in the region studied. We see the rate change by a factor of only 1.5 (Table 1).

The set of equations can be equally well fit assuming an acetic reaction order of 0 or 0.5 and a compensation effect of 1.15 or 1.28, resp. This shows that the adsorption of HOAc is strong but does not limit the reaction rate. This result, in addition to the sharp drop in reaction barrier with increasing acid pressure, implies surface alteration due to compound formation. Therefore, the change in rate with increasing HOAc pressure can be accounted for by a change in the rate constant alone. This is demonstrated in Fig. 1, where the observed rate parallels the calculated rate constant very closely. The following results from DRIFTS–MS support the existence of a surface acetate compound.

B. Temperature-Programmed Reactions; DRIFTS–MS

Figure 3 contains DRIFTS spectra in the 2000–1100 cm^{-1} region of a catalyst under steady-state conditions (upper spectrum) and after removal of HOAc and C_2H_4 from the gas phase (lower spectrum). Peak assignments are made from spectra of the individual components in the DRIFT cell (Fig. 4). The two sets of three peaks centered at approximately 1890 and 1445 cm^{-1} result from gas phase ethylene, and are due to the P, Q, and R branches of the $\nu_7 + \nu_8$ combination bands and the ν_{12} fundamental band, resp. (*16*). The spectrum of HOAc exhibits a doublet at 1790 and 1770 cm^{-1}. Although the band at 1790 cm^{-1} has not previously been assigned, the 1770-cm^{-1} band results from a carbonyl stretch of monomeric HOAc vapor (*17*). In all of our studies the intensity of the 1790-cm^{-1} band parallels that of the 1770-cm^{-1} band, so we conclude this band is also related to the gas-phase monomer. A third band at 1735 cm^{-1} also arises from the carbonyl stretch of HOAc. This has been shown to result from the dimer. The band at 1420 cm^{-1} is assigned to asymmetric CH_3 bending, and those at 1290 and 1170 cm^{-1} are due to a single bond C–O stretch and an O–H bend (*17*). Palladium acetate is formed on the catalyst surface under steady state conditions. Its asymmetric carboxylate stretch appears at 1607 cm^{-1}, and that of the symmetric stretch falls at 1433 cm^{-1}. Absorption from the po-

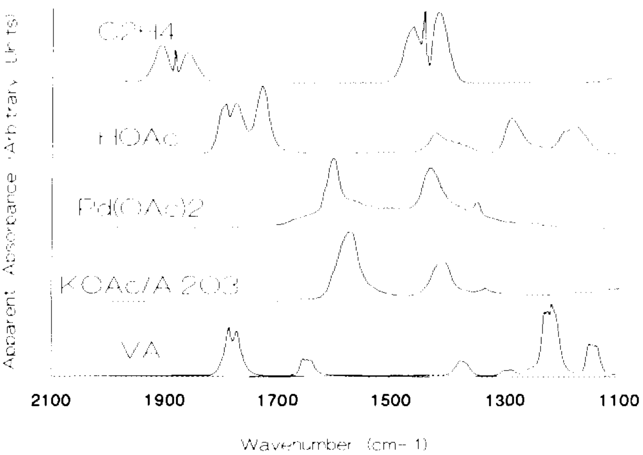

FIG. 4. Diffuse reflectance infrared absorption of system components. They are presented in the order of ethylene, acetic acid, palladium acetate, potassium acetate deposited on alumina, and vinyl acetate from top to bottom, respectively.

tassium acetate promoter is also visible at 1575 cm^{-1} (asymmetric stretch) and 1410 cm^{-1} (symmetric stretch) (*18*). The two metal acetates also exhibit absorptions at 1352 cm^{-1} ($Pd(OAc)_2$ and 1335 cm^{-1} (KOAc) (Fig. 4). The alumina substrate does not interfere in the region of interest. Vinyl acetate shows a pair of overlapping peaks at 1787 and 1774 cm^{-1} (carbonyl stretch), a broad absorption at 1651 cm^{-1} (C=C stretch), and two absorptions at 1220 and 1152 cm^{-1} (C–O– single bond vibrations) (*19*). Vinyl acetate is present in very small concentrations in the reaction and its individual absorptions are likely to be hidden by those of HOAc (Figs. 3 and 4).

When the gas phase reactants are sequentially replaced by N_2, (as described in the Methods section) the peaks assigned to ethylene, HOAc monomer, and VA disappear (Fig. 3, lower spectrum). The absence of these species in the gas phase is confirmed by the mass spectrum. The peaks due to the metal acetates remain as do three other peaks at 1735, 1270, and 1230 cm^{-1}. Of the latter three the high-frequency peak is indicative of a carbonyl stretch, while the lower two are associated with C–O– single bond stretch. The three together suggest the presence of saturated esters (*19*). The absence of any hydrocarbon species in the gas phase indicates that these bands result from surface bound species. A more complete assignment of these three peaks will follow after all the DRIFTS–MS evidence has been presented.

Each of the reagents analyzed exhibit a sharp "fingerprint" absorption in the range of 2000–1500 cm^{-1}. Hence, for reasons of clarity all but one (see Fig. 6) of the DRIFTS–MS figures will display this smaller region.

A TPRxn in a flow of 10% O_2 in C_2H_4 reveals that the peaks at 1735, 1270, and 1230 cm^{-1} are associated with VA and HOAc formation (Figs. 5 and 6). Vinyl acetate forms from 100–180°C, with the maximum rate occurring at 146°C. Over the temperature range 100–160°C the DRIFTS spectra change little except a small, but reproducible decrease in the band at 1735 cm^{-1} (Fig. 5). A broader temperature range (Fig. 6) shows this band, the two at 1270 and 1230 cm^{-1}, and the band assigned to $Pd(OAc)_2$ to be severely attenuated with the formation of acetic acid from 155–215°C. The maximum rate occurs at ca. 200°C. Further formation of HOAc at higher tempera-

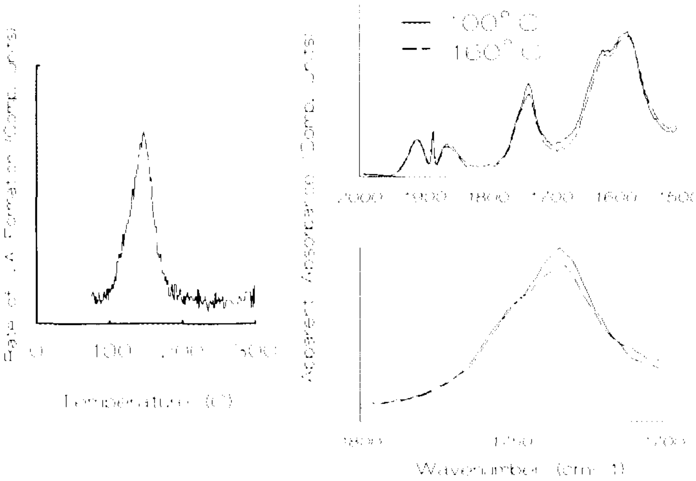

FIG. 5. Temperature programmed reaction of ethylene and oxygen with acetic acid activated on a Pd catalyst. The solid IR spectrum is taken at 100°C. The dotted spectrum is taken at 160°C.

tures (>230°C, maximum rate at ca. 295°C) results from the destruction of the KOAc promoter phase.

The presence of Pd(OAc)$_2$ during VA synthesis has been previously noted (*7*, *8*). Indeed, Pd(OAc)$_2$ can be used as a catalyst precursor in both the homogeneous (*20*) and heterogeneous (*21*) vinyl acetate catalyst systems. DRIFTS–MS studies show that it appears with the establishment of steady state and is destroyed with the formation of gas-phase vinyl acetate and acetic acid in TPRxn's. Therefore, we decided to study the bulk compound with temperature-programmed DRIFTS–MS experiments. As discussed above, 5% Pd(OAc)$_2$ is physically mixed with KCl in the DRIFTS cell, and a TPRxn with the O_2/C_2H_4 mixture is run.

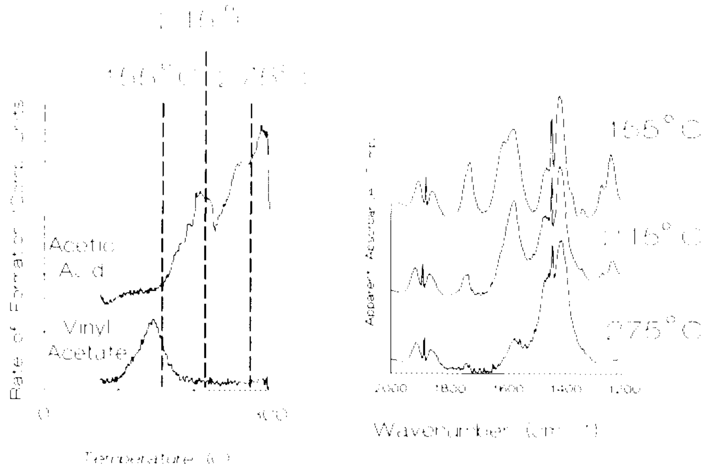

FIG. 6. Temperature programmed reaction of ethylene and oxygen with acetic acid activated on a Pd catalyst. The upper IR spectrum is taken at 155°C, the middle spectrum at 215°C, and the lower spectrum at 275°C.

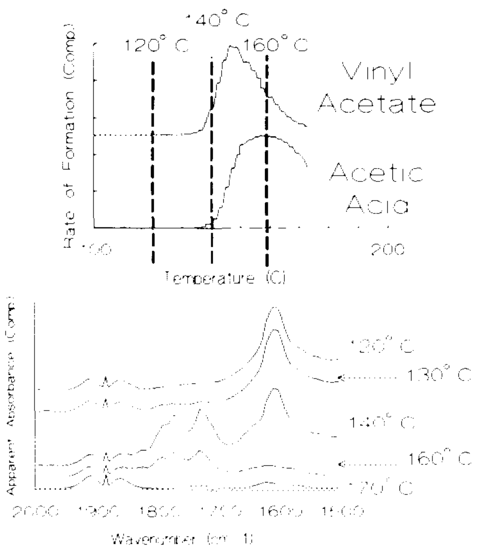

FIG. 7. Temperature programmed reaction of ethylene and oxygen with palladium acetate. The IR spectra are taken at 120, 130, 140, 160, and 170°C from top to bottom, respectively.

The DRIFTS–MS results are presented in Fig. 7. This study confirms that vinyl acetate can be produced by this reaction and it is evolved in the range 130–170°C. Acetic acid is also seen at temperatures above 140°C. The DRIFTS spectra show what is occurring at the surface. At 120°C only peaks from gas-phase ethylene (<1800 cm^{-1}) and solid Pd(OAc)$_2$ (1607 cm^{-1}) are visible. Two sets of peaks due to gas-phase acetic acid (1800–1760, and 1735 cm^{-1}) become visible when the reaction begins to make vinyl acetate at 130°C. The surface species absorbing at 1735 cm^{-1} is also present (see below). These peaks grow in and become pronounced at the point HOAc appears in the mass spectrometer at 140°C. The growth in these peaks correlates with a loss of absorption from Pd(OAc)$_2$. At the maximum rate of HOAc formation at 160°C the peak resulting from Pd(OAc)$_2$ is greatly attenuated. By 170°C the reaction is almost complete, and very little absorption from acetate species is visible in the IR.

The surfaces of the Pd(OAc)$_2$/KCl mixture and the Pd catalyst appear very similar when making vinyl acetate. This comparison is presented in Fig. 8. The upper spectrum is of the catalyst surface as it is quenched from steady state. The lower two spectra are of the mixture. The middle is taken after the TPRxn is quenched at peak vinyl acetate production. The lower is after the reaction is almost complete. All are taken after no gas-phase reagents are detectable in the mass spectra and individually contain what may be called the primary surface components. Each shows evidence of the group of species centered at 1735 cm^{-1} that is associated with the formation of vinyl acetate and acetic acid in the TPRxns. The absorption from Pd(OAc)$_2$ at 1607 cm^{-1} is also common. An interesting observation is that the absorption associated with KOAc (1575 cm^{-1}) is clearly visible in the Pd(OAc)$_2$/KCl mixtures. This suggests an interaction between the Pd(OAc)$_2$ and the dispersing KCl matrix occurs to form the catalyst promoting phase. In fact, we have reported that the location and size of the vinyl acetate peak in the TPRxn is strongly influenced by the nature of the dispersing matrix (*2*).

C. Assignment of the Absorption at 1735 cm^{-1}

To our knowledge, the absorption of a Pd bound carbonyl species at 1735 cm^{-1} has not been observed. Although, it has been reported that a form of catalytically active palladium acetate does absorb in the region from 1600 to 1750 cm^{-1} (*22*). The absence of companion HOAc peaks at 1790 and 1770 cm^{-1} and the lack of detection by the mass spectrometer eliminates gas-phase HOAc as a possible cause of this band. Physisorbed or condensed HOAc are also ruled out since the associated vapor pressure (HOAc boils at 118°C) would yield detection in the gas phase. None of the other gas-phase reagents nor the surface acetates exhibit a band here. These observations, along with the appearance of this band during reactions involving Pd(OAc)$_2$, imply that it results from some

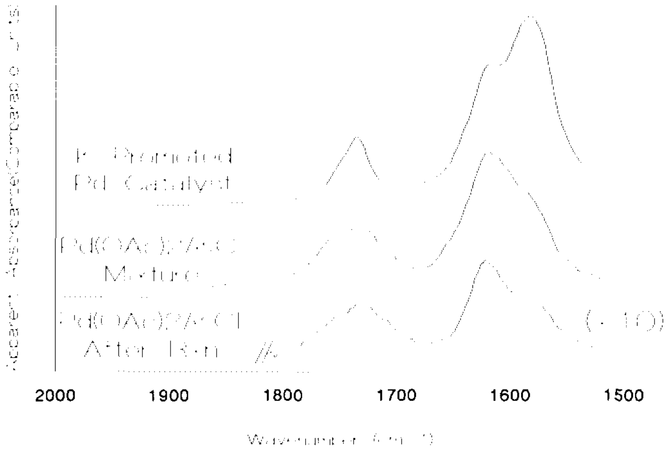

FIG. 8. Comparison of an active catalyst surface with an "activated palladium acetate/potassium chloride mixture. The upper spectrum is of the potassium promoted Pd catalyst, the middle spectrum is of the $Pd(OAc)_2/KCl$ mixture quenched during reaction, and the lower spectrum is of the same mixture after reaction.

form of acetic acid (or acetate) bound to the surface of Pd crystallites.

The question arises as to whether this peak is simply an acetic fragment, or if it has an ex-ethylene group associated with it. The peak forms under steady state conditions in which oxygen, acetic acid, ethylene and vinyl acetate are present in the gas phase. However, it remains stable after the latter two are purged from the system at 140°C. A TPRxn with C_2H_4 and O_2 causes its slight attenuation as VA is being measurably produced at temperatures below 120°C (Fig. 5). So it appears that addition of gas phase ethylene is necessary for the reaction pathway to be completed. It would be hard to imagine that an unsaturated ethylene (either π or di-σ bonded) species would possess a long residence time on a Pd surface under these oxidizing conditions (*23*). This would be particularly true for an ethylene group activated at the vinyl position by an ester linkage. Indeed, inspection of the spectra in the olefin CH stretching region from 3050–3000 cm^{-1} shows no peaks.

The issue of structure remains. The data and supporting evidence appear to show that this species possesses a carbonyl absorption, is bound to Pd and is probably not associated with ethylene. Additional information comes from the absorption bands falling between 1280 and 1230 cm^{-1}. As stated above, bands falling in this region can be assigned to C–O– stretching vibrations (*19*). The temperature-programmed DRIFTS experiment in Fig. 6 shows these to be attenuated with the $Pd(OAc)_2$ bands and the band at 1735 cm^{-1}. This occurs as HOAc and VA are formed in the reaction. We know these bands are not due to $Pd(OAc)_2$ (Fig. 4), so we associate them with the 1735-cm^{-1} peak. The three taken together strongly suggest that the adsorbed species is either a carboxylic acid or an ester group. If the species is bonded to the surface with the carbonyl function intact, it only makes sense that dissociative bonding occurs at the carboxylate–acidic hydrogen linkage. We have seen that injection of HOAc into an oxygen flow over a catalyst at 140°C does result in adsorption and water evolution. Therefore, we conclude that this band results from a carbonyl absorption of an acetic acid conjugate base (acetate) bonded to a Pd surface. Structurally it would look like a "Pd-ester," but charge transfer arguments would call it a Pd acetate. Of course, this species needs to be distinguished from the "typical" bidentate palladium acetate bond possessing two C–O bonds of 1.5 order and a high degree of electron delocalization (*24*). Again, the latter species displays characteristic infrared absorbances at 1607 and 1433 cm^{-1} (Fig. 4).

D. Temperature-Programmed Reactions; Quantitative Studies

The qualitative similarities between the surfaces of Pd catalysts and $Pd(OAc)_2/KCl$ mixtures under reaction conditions are remarkable. In light of the effect HOAc has on the reaction barrier (Fig. 2) it would seem strong adsorption of HOAc precedes surface $Pd(OAc)_2$ compound formation. An important difference between the catalyst and model systems is, however, the temperatures in the TPRxns at which VA is formed. Therefore, it would be useful to know the apparent activation energy (Ea) for this process in each system. If the energetics for VA formation in both are the same, then $Pd(OAc)_2$ may be an adequate model of an active catalyst. If not, alterations to the model must be made.

We have shown that VA forms during TPRxns as a result of combining C_2H_4 and O_2 with a specific surface species. To determine the activation energy in each system we first assume that the reaction order of this surface species is one. It is also assumed that all of this species does in fact convert to VA. For this to be true then the surface species that form VA and HOAc must necessarily be unique. The O_2 and C_2H_4 concentrations are in large excess and constant in the reactions, so they can be incorporated into the pre-exponent. The following kinetic expression results:

$$\frac{d[\mathrm{VA}]}{dt} = A' \exp(-E_a/RT)[\mathrm{S}].$$

Here [S] is the concentration of the acetate surface species. Taking the derivative with respect to temperature and simplifying yields

$$\frac{d[\mathrm{VA}]}{dT} = (E_a/RT^2)[\mathrm{S}] \bigg/ \left(1 + \frac{\mathrm{FR}}{A' \exp(-E_a/RT)}\right).$$

The factor FR in this expression represents the reagent flow rate.

The equation (dotted line) is fit to TPRxn's using an iterative approach. Comparisons of this fit with experimental data for a Pd catalyst and the $Pd(OAc)_2/KCl$ mixture are contained in Fig. 9. Two further profiles from a $Pd(OAc)_2/KOAc$ mixture and $Pd(OAc)_2$ deposited on a Pd catalyst are in Fig. 10. The fits are satisfactory, indicating that our assumptions are reasonable.

The fitted equations show (Table 2) that the apparent activation energies are considerably different between the catalyst (37 kcal/mol) and the bulk acetate (93 kcal/mole). This difference between the samples is at first surprising given the similarities apparent in the DRIFTS–MS study. Several factors may contribute. But first, the role of Cl^- should be addressed. Chlorine is not present in the supported catalyst, but it is very abundant in the mixture. To determine if the presence of Cl^- destabilizes the transition state, a mixture of $Pd(OAc)_2/KOAc$ was studied. This TPRxn gave an even higher activation energy (129 kcal/mole), so Cl^- should not be regarded as a problem in these particular reactions.

A likely factor in the difference of E_a's is the nature of the two materials. First, a bulk compound like $Pd(OAc)_2$ should, as a general rule, exist at a lower energy level than a surface species on a catalyst. The compound has a low surface area with most acetate and Pd being highly coordinated. Conversely, the very purpose of a catalyst is to use surface coordinative unsaturation to activate reagents. Second, on the catalyst the $Pd(OAc)_2$-like active phase is probably intimately associated with Pd metal or oxide. The ratio of VA produced during the TPRxn to Pd present on the catalyst is less than .025 (Table 2). This shows that a large amount of Pd is not directly participating in

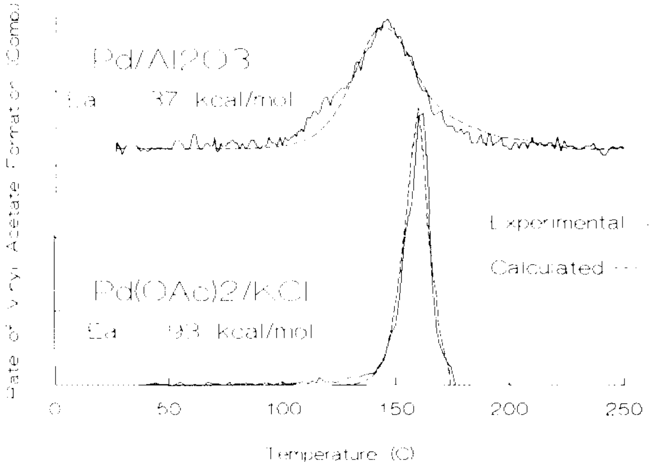

FIG. 9. Temperature-programmed reaction profiles of the reaction of ethylene and oxygen with surface activated acetic acid species. The solid lines are the experimental results and the dotted lines represent the calculated fit. The upper profile is of acetic activated on a Pd catalyst; the lower profile is of a Pd(OAc)$_2$/KCl mixture.

the reaction. It would be unrealistic to expect that abundant Pd or PdO species do not influence a reaction occurring on a supported catalyst. As a means to investigate this we deposited Pd(OAc)$_2$ on top of a Pd catalyst. The peak maximum from the ensuing TPRxn falls at a higher temperature than in the case of the Pd(OAc)$_2$/KCl mixture (Table 2). Yet, the fit from the kinetic expression yields the lower activation energy of the two at 70 kcal/mole. This result is, at first, curious. It is almost second nature to expect reactions occurring at higher temperatures to possess higher activation barri-

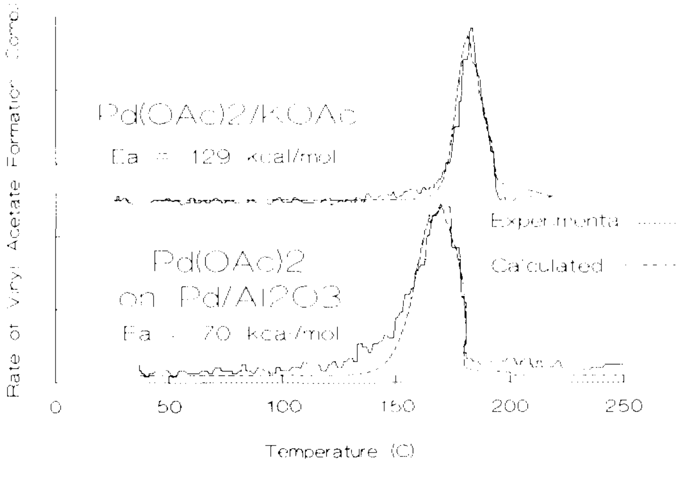

FIG. 10. Temperature-programmed reaction profiles of the reaction of ethylene and oxygen with surface-activated acetic acid species. The solid lines are the experimental results and the dotted lines represent the calculated fit. The upper profile is of a Pd(OAc)$_2$/KOAc mixture; the lower profile is of Pd(OAc)$_2$ deposited on Pd/Al$_2$O$_3$.

TABLE 2

Parameters Derived from TPRxn of Acetic Surface Species on Different Media with 10% O_2/C_2H_4

Catalyst or media	Rate maximum (°C)	E_a (kcal/mole)	VAM/Pd (× 100)
Pd/Al_2O_3	146	37	2.41
$Pd(OAc)_2/KCl$	163	93	7.68
$Pd(OAc)_2/KOAc$	184	129	3.76
$Pd(OAc)_2$ on Pd/Al_2O_3	174	70	0.494

ers. However, a very extensive study correlating temperature-programmed reduction profiles with kinetic parameters has shown that peak shape is equally important in determining activation energy (*25*). The lower barrier over the acetate covered catalyst relative to the alkali mixture results from the greater breadth of its TPRxn peak. The drop in E_a supports the proposal that Pd metal or oxide does indeed interact with $Pd(OAc)_2$ in producing the active site. Pd metal also forms in the TPRxn of bulk $Pd(OAc)_2$, but only after a considerable degree of reaction. To summarize, the active phase in VA synthesis is some form of surface $Pd(OAc)_2$ intimately associated with Pd metal or oxide.

CONCLUSIONS

The strong interaction between Pd and HOAc leads to surface compound formation which acts to lower the reaction barrier. DRIFTS–MS shows that $Pd(OAc)_2$ forms on the catalyst surface under reaction conditions. Compound formation is consistent with kinetic results which suggest an acetic reaction order of 0. Solid $Pd(OAc)_2$ when reacted with an O_2/C_2H_4 mixture also makes VA. In this state the surface looks very similar to that of an active catalyst within the carboxylate IR region. Significant peaks at 1575 cm^{-1} (KOAc), 1607 cm^{-1} ($Pd(OAc)_2$), and 1735 cm^{-1} are common to each. The difference between the two systems is the activation barrier to the formation of VA from the surface activated acetic species. The value for the active catalyst is well below that for the $Pd(OAc)_2/KCl$ mixture. This difference is due, in part, to the presence of Pd metal or metal oxide interacting with the active site. In conclusion, the surface phase active for VA synthesis consists of islands of $Pd(OAc)_2$-like species on top of Pd metal or oxide crystallites.

REFERENCES

1. Highfield, J. G., Prairie, M., and Renken, A., *Catal. Today* **9,** 39, (1991); White, R. L., *J. Anal. Appl. Pyrol.* **18,** 325 (1991); Basini, L., Marchionna, M., and Aragno, A., *J. Phys. Chem.* **96,** 9431 (1992).
2. Blitz, J. P., and Augustine, S. M., *Appl. Spectrosc.* **45,** 1746 (1991).
3. Robinson, R. E., U.S. Patent 3,190,912 (1965).
4. Samanos, B., Boutry, P., and Montarnal, R., *J. Catal.* **23,** 19 (1971).
5. Debellefontaine, H., and Besombes-Vailhe, J., *J. Chim. Phys.* **75,** 801 (1978).
6. Wieland, J. H., Prauser, G., and Dialer, K., *Chem. Ing. Technol.* **54,** 605 (1982).
7. Nakamura, S., and Yasui, T., *J. Catal.* **17,** 366 (1970).
8. Nakamura, S., and Yasui, T., *J. Catal.* **23,** 315 (1971).
9. Griffiths, P. R., and de Haseth, J. A., "Fourier Transform Infrared Sectroscopy," p. 544. Wiley, New York, 1986.
10. Lum, D. W., German Patent 1,944,933 (1970).
11. Kortüm, G., "Reflectance Spectroscopy," p. 59. Springer-Verlag, New York, 1969.
12. Murthy, R. S. S., Blitz, J. P., and Leyden, D. E., *Anal. Chem.* **58,** 3167 (1986).
13. Levenspiel, O., "Chemical Reaction Engineering," p. 488. Wiley, New York, 1972.
14. Bond, G. C., "Catalysis by Metals," p. 139. Academic Press, London, 1962.

15. Bond, G. C., "Catalysis by Metals," p. 384. Academic Press, London, 1962.
16. Herzberg, G., "Infrared and Raman Spectra," p. 326. Van Nostrand, New York, 1945.
17. Weltner, W., Jr., *J. Am. Chem. Soc.* **77,** 3941 (1955).
18. Spinner, E., *J. Chem. Soc.*, 4217 (1964); Kagarise, K. E., *J. Chem. Soc.* **59,** 271 (1955).
19. Bellamy, L. J., "The Infra-red Spectra of Complex Molecules," p. 204. Chapman and Hall, London, 1975.
20. Henry, P. M., *J. Org. Chem.* **38,** 1681 (1973).
21. Wunder, F., Quadflieg, T., Roscher, G., and Heck, G., U.S. Patent 4,370,492 (1983).
22. Kuznetsova, N. I., Fedotov, M. A., Likholobov, V. A., and Yermakov, Yu. I., *J. Mol. Catal.* **38,** 263 (1986).
23. Stuve, E. M., and Madix, R. J., *Surf. Sci.* **160,** 293 (1985).
24. Barton, D. H. R., Khamsi, J., Ozbalik, N., Ramish, M., and Sarma, J. C., *Tetrahedron Lett.* **30,** 4661 (1989).
25. Monti, D. A. M., and Baiker, A., *J. Catal.* **83,** 323 (1983).